

DECISION MAKING COMPONENTS IN CYCLISATION OF MANNOSE DERIVATIVES – A COMPUTATIONAL APPROACH

M. Rakhila¹, KR. Jinuraj², M. Dhanalakshmi³, D. Reshmi⁴,
Andrew Titus Manuel⁵ and UC. Abdul Jaleel^{6*}

^{1,2,3}Research and Development Centre, Bharathiar University,
Marudhamalai Rd, Coimbatore, Tamil Nadu – 641 046, India.

^{4,5}OSPF NIAS Drug Discovery Lab, NIAS, Indian Institute of Science Campus,
Bengaluru, Karnataka – 560 012, India.

⁶Principal Scientist, Cheminformatics, OSPF NIAS Drug Discovery Lab, NIAS,
Indian Institute of Science Campus, Bengaluru, Karnataka – 560 012, India.

ABSTRACT

The components responsible for deciding the conformational stability of mannose - Schiff base derivatives were analyzed. Based on the hydrogen bond donating ability and hydrogen bond accepting ability, a virtual derivative series was designed. Various levels of theories were adopted to elucidate the energy points on the potential energy surface of the molecules and different energy components using molecular mechanics MM+, Semi-empirical AM1 and PM3, 6-311++G** under B3LYP level of theory of Density Functional Theory (DFT). Hydrogen bonding ability, electrostatic potential and molecular energy were found to be the decisive principal components in the conformational stability of mannose - Schiff base derivatives. MM+, AM1 and DFT could provide a trend that was utilized to validate the conformational stabilities that had been provided by crystallographic studies for the four derivatives of D-mannose.

Keywords: DFT, semi-empirical, molecular mechanics, Schiff base, electrostatic potential.

INTRODUCTION

Schiff bases play a decisive role in multi-dentate chelating which have immense applications in the area of asymmetric catalysis¹, synthesis of stereo-selective alpha amino acids², selective catalytic activity³, biological catalysis⁴, as a drug designing diagnostic tool^{5,6,7} and as an anticonvulsant⁶. Thus, by predicting the conformational stability, it is possible to elucidate the complexing nature of this class of ligands in coordination compounds. Mannose Schiff base derivatives are significant due to their properties like anti-parasitic, anti-viral, anti-bacterial and anti-fungal properties^{8,9,10}.

Conformational studies based on crystallographic results of D-mannose - Schiff base derivatives had been provided by Ojala et al¹¹. A theoretical understanding for the

experimentally validated results of Ojala et al were studied by adopting various computational levels of theories; molecular mechanics MM+, Semi-empirical AM1 and PM3 and 6-311++G** under B3LYP level of theory of Density Functional Theory (DFT). Molecular mechanical method¹² based on Newtonian Mechanics, primarily depends on the force field equations. This equation connects various structural parameters like bond angle, dihedral angle, bond distance, van der Waals interactions and electrostatic interactions with the energy of the molecular system. Among various functional forms of molecular mechanical methods (AMBER, CHARMM, OPLS and BIO+), MM+¹³ was adopted as it contains both quadratic and cubic stretch terms¹⁴. Wherein, the cubic term

supports a more realistic view of the molecule with lesser approximation.

$$E_{\text{quadraticstretch}} = K_r (r - r_0)^2$$

Where:

K_r – force constant

r_0 – equilibrium constant

r - Distance

$$E_{\text{bond}} = 143.88 \sum_{\text{bonds}} \frac{1}{2} K_r (r - r_0)^2 [1 + CS(r - r_0)]$$

Where:

$r-r_0$ – cubic stretch term

CS – cubic stretch term constant

K_r – force constant

Cubic stretch term specifically connects the bond distance with the molecular energy of the system during the minimization and optimization processes more precisely. The cubic stretch term in MM+ force field, would make it possible to envisage the bond distance that is obtained from the XRD studies in an accurate way.

A characteristic feature of MM+ force field is the unique way in which dipole moment calculations are done. The electrostatic contribution comes from defining a set of bond dipole moments that are associated with polar bonds and not from the usual contribution of electrostatic charge-charge interactions. These bond moments are defined along the bond stretching parameters. The center of the dipole is expressed to be the midpoint of the bond and the two dipoles μ_i and μ_j which are separated by R_{ij} .

The MM+ dipole interaction energy is:

$$E_{\text{dipole}} = 14.39418 \epsilon \sum_{i,j \in \text{polar bonds}} \mu_i \mu_j \left[\frac{\cos(\chi) - 3\cos\alpha_i \cos\alpha_j}{[R_{ij}]^3} \right]$$

Where:

ϵ - dielectric constant

μ_i and μ_j – respective dipoles under study

R_{ij} – is the resultant vector of the two dipole vectors that make an angle α_i and α_j

χ - Angle between the two dipole vectors

The constant 14.39418 is the unit conversion constant from ergs/molecule to kcal/mol.

Another unique feature available in MM+ is the sextic equation which is quite essential for understanding the displacement from equilibrium during the deformation of an angle from its normal value. As a harmonic function is used in this calculation, it would be possible to get meaningful insights into systems having a large number of atoms especially the case being that our study deals with comparatively large number of atoms.

The primary equation is:

$$E_{\text{bondangle}} = \sum_{\text{angles}} K_\theta (\theta - \theta_0)^2$$

Where

K_θ – bending force constant

θ_0 – equilibrium value

θ – Displacement from equilibrium value

And the sextic equation is:

$$E_{\text{bondangle}} = 0.043828 \sum_{\text{angles}} \frac{1}{2} K_\theta (\theta - \theta_0)^2 [1 + SF(\theta - \theta_0)^4]$$

$$E_{\text{dihedral}} = \sum_{\text{dihedrals}} \frac{V_1}{2} (1 + \cos \phi) + \frac{V_2}{2} (1 - \cos 2\phi) + \frac{V_3}{2} (1 + \cos 3\phi)$$

Where:

Φ – Dihedral angle

The above equation was used to calculate the dihedral angle in MM+. Though it is not a unique feature pertaining to MM+ alone, it was useful in trying to understand the underlying principles between symmetry and conformations from the torsion energy interactions that were obtained on solving the above said equation.

V_1 , V_2 , and V_3 are the torsional force constants.

In this study, van der Waals was the most studied parameter, as the primary hypothesis in this study was that hydrogen bonding and van der Waals interactions do play a pivotal role in deciding the cyclisation process of a molecule. So, it is imperative that these parameters were studied in detail.

In MM+, these interactions are studied by using a combination of an exponential repulsion, with an attractive $(1/R)^6$ dispersion interaction instead of using Lennard-Jones potential.

The van der Waals interaction was then calculated as:

$$E_{\text{van der Waals}} = \sum_{i,j \in \text{vdW}} \epsilon_{ij} (2.9 \times 10^5 e^{-12.5 \rho_{ij}}) - (2.25 \rho_{ij})^{-6}$$

The van der Waals radius, $r_{ij}^* = r_i^* + r_j^*$, the hardness parameter $\epsilon_{ij} = \sqrt{\epsilon_i \epsilon_j}$ (ϵ_i determines the depth of the attraction and how to push atoms close together).

And $\rho_{ij} = R_{ij}/r_{ij}^*$

The above-mentioned parameters are given prime importance in MM+ calculations. Hence one of the focus in this study was to carry out molecular mechanics (MM+) calculations to elucidate the decisive role that these varying parameters play during the cyclisation of a molecule.

Molecular mechanics is considered to be the best tool for predicting the geometry, the heat of formation and the conformation of a molecule. But during the course of this study, there arose an interest to enquire about the prediction power of Hartree-Fock formalism, utilizing Semi-empirical calculation methods. Our inquisitiveness was to calculate/compare the Semi-empirical results with molecular mechanics and XRD data, as Semi-empirical way of computational methods can be used to predict electronic properties of molecules, such as dipole moment and spectroscopy. During the calculation, Semi-empirical methods consider only valence electrons and it usually omits many electron-electron interaction integrals as they are negligible. To compensate for neglecting the overlapping integrals, Semi-empirical methods were introduced based on molecular data based parameters. The most commonly used Semi-empirical methods as well as that offers the most reliable predictions for heats of formation, ground state geometries and ionization potentials are AM1 and PM3. The parameterization method is based upon the Hartree-Fock formalism. The Semi-empirical methods AM1 and PM3 make use of minimal valence basis sets of Slater type orbitals^{16,17}. Also, both these Semi-empirical methods use comparatively fewer parameters than molecular mechanics method. So, in this study we used AM1 and PM3 semi empirical methods.

The backbone of quantum mechanics lies in the solution of time independent non-relativistic formalism of Schrodinger equation. But while considering many electrons many atom systems, it was found to be inept in solving the Schrodinger equation by using the wave function. Thus, it was necessary to utilize density functional analysis for solving the many electrons many atom systems problems.

In this study we used 6-311++G** under B3LYP level of theory of DFT, as it incorporates generalized gradient approximations (GGA) and local density approximations (LDA) which yields an improved DFT mathematics and useful features of ab-initio methods such as Hartree-Fock method.

$$E[\rho] = T[\rho] + E_{ee}[\rho] + E_{Ne}[\rho]^{14}$$

T - Kinetic energy

EE - electron electron repulsion

Ne - nuclei-electron attraction

As the exact functionals for DFT exchange and correlation functionals are known only for a free electron gas, approximations such as the LDA and GGA are used for molecular calculations¹⁸. LDA functional depends only on

the density at the coordinates where the functional is evaluated. Whereas, GGA although like LDA, it also takes into consideration the gradient of the density. Hence GGA functionals are considered to be more accurate than LDA functionals.

MATERIALS AND METHODS

Molecular mechanical calculations were done using HyperChem 8.0 Computational Chemistry package¹⁹. The molecule obtained was minimized by using Polak-Ribiere optimizer. Similarly, all the Semi-empirical and DFT computations were made. PM3 and AM1 methods were used for Semi-empirical methods and 6-311++G** under B₃LYP level of theory of DFT were used. Electrostatic potential, bond energy, van der Waals interactions and dihedral energies were generated. Values of dipole moment were calculated for all the methods namely PM3, AM1 and 6-311++G** under B3LYP level of theory of DFT methods.

Molecular Mechanical Calculations

The studies were carried out using Molecular Mechanical calculations utilizing MM+ force field available in HyperChem 8.0. Optimization was based on Monte Carlo method. This resulted in a range of conformations with varied torsional angle. The method enlisted the use of T=300K to 400K. The resulting molecule was then minimized by using Polak-Ribiere optimizer. Termination of molecule minimization was done, when gradient root mean square went below 0.01 kcal/mol and it was carried out based along the following criteria: -

- ✓ Conformational search based on simulated annealing method with heat time 0.1ps, runtime 0.5 ps, cool time 0.1 ps, starting temperature 100 K and temperature of simulation 300 K with a temperature step 30 K as described by Choe et al²⁰.
- ✓ The structure obtained was then verified utilizing IR spectrum so as to verify that no negative frequencies were present in the vibration spectrum. HyperChem 8.0 was used for simulating along with the computational methods that were adopted.

Semi-empirical Calculations

Determination of molecular stability was also studied by enlisting PM3 that is a semi empirical calculation. MM+ force field and Polak-Ribiere optimizer were initially applied on the molecule constructed using HyperChem 8.0 GUI. After which PM3 method

was applied on the molecule. Another Semi-empirical method AM1 was also applied on all the molecules. As it is in the case of MM+ calculations, all the parameters referred to here are for isolated molecules in vacuum.

DFT Calculations

Density Functional Theory (DFT) was adopted for this calculation by using 6-311++G** under B3LYP level of theory.

Training Set

A virtual derivative series was designed based on hydrogen bond acceptors and hydrogen bond donors and their substituents are listed in Table 1 to interpret the rationale that could be responsible for the cyclisation. Concomitantly investigations were also carried out to examine whether any significant trends could be realized if there does exist a correlation between hydrogen bond interactions, dipole moment, electrostatic potential and total molecular energy with the mannose - Schiff base derivatives conformational stabilities.

An experimental set of mannose derived Schiff base (probe molecules), D mannose oxime (MO), N-mannopyranosylsemicarbazide(MPS), phenylmannopyranosylamine (PMS) and N-p chlorophenylmannopyranosylamine (CMA) that exist in both conformations: - acyclic as well as cyclic, prepared by Ojala et al, listed in Table 2 were collected so as to investigate the rationale behind cyclisation.

RESULTS AND DISCUSSIONS

Molecular mechanics MM+ force field was applied on the virtual derivative series based on the rationale that hydrogen bond donating ability and hydrogen bond accepting ability does play a role in the selection of cyclic conformation of the molecule. The derivative series was developed from the cyclic and acyclic conformations of D-mannose that is depicted in Figure 1. And it was designed in the order of zero hydrogen bond donors, poor hydrogen bond donors, moderate hydrogen bond donors, good hydrogen bond donors, strong hydrogen bond donors, very strong hydrogen bond donors, zero hydrogen bond acceptors, moderate hydrogen bond acceptors and very strong hydrogen bond acceptors. A range of properties like bond energy, stretch bend energy, angle energy, van der Waals energy, dihedral energy and electrostatic potential were studied which are listed in Table 2 and Table 3. Among these different energy components that were studied, a gradation for electrostatic potential obtained as shown in Figure 2. A particular pattern was observed for hydrogen bond donor class and for hydrogen

bond acceptors. The pattern observed was just the reverse. On comparing the cyclic and acyclic conformations, it was observed that the electrostatic potential was the highest for acyclic when compared to cyclic on considering the hydrogen bond donor class. In the case of hydrogen bond acceptor class, acyclic conformation was observed to have the lowest value of electrostatic potential when compared to the cyclic conformations. From the parameters observed from the two classes of the derivative series; was that among the two conformations of a molecule, the one with the lowest electrostatic potential was preferred over the other. This helped in understanding that cyclisation was being favored as hydrogen bond donating ability increased.

For further substantiating our observation behind the rationale, Semi-empirical methods AM₁ and PM₃ were applied. PM₃ method did not provide any justifiable gradation that supported our rationale other than just verifying that no negative frequencies were present in the vibration spectra. Besides, AM₁ method provided a gradation in property with respect to energy points on the potential energy surface of the molecules as shown in Figure 3.

As mannose derived Schiff base exist in both conformations: - acyclic as well as cyclic and according to Ojala et al, it was confirmed by XRD that D mannose oxime (MO) to be acyclic in nature, whereas for N-mannopyranosylsemicarbazide (MPS), n-phenylmannopyranosylamine (PMS) and N-p chlorophenylmannopyranosylamine (CMA) to be cyclic. The methods adopted to elucidate the rationale behind the role played by hydrogen bond accepting ability and hydrogen bond donating ability were then applied to the experimental series of Ojala et al and the results are listed in Table 4, as shown in Figure 4 and 5. Among the conformations, cyclisation was favored when intra-molecular hydrogen bond interactions increased as shown in Figure 6. But the most stable confirmation that was observed was the molecule with the least electrostatic potential and least total molecular energy. So as to substantiate the trend obtained with regard to electrostatic potential, an electrostatic potential contour representation was investigated and its representation is shown in Figure 7.

Coherence regarding the rationale that hydrogen bond donating or accepting ability plays a decisive role in the cyclisation were further obtained by applying 6-311++G** under B3LYP level of theory of DFT. Gradation in energy was observed with respect to energy coordinate points on the potential energy surface of the molecules as shown in Figure 8.

But DFT studies could not validate the conformational stability of the MPS molecule in comparison to other levels of theories. DFT studies provided a gradation in property in intra-molecular hydrogen bonds also. When the number of intra-molecular hydrogen bonds increased, it was found that it favored cyclisation. No significant results were obtained with regard to dipole moment from the virtual derivative series and also from the experimentally validated series of Ojala et al.

CONCLUSION

The study could predict in elucidating the components influencing the cyclisation process. The principle factors for the cyclisation process for mannose based Schiff bases of Ojala et al depends on the following: - electrostatic potential, total energy and intra-molecular hydrogen bonding. Also, from the virtual reactive series along with the experimentally validated series of Ojala et al, the most preferable conformation will have the least electrostatic potential, the least total energy and the maximum number of intra-molecular hydrogen bonding.

AUTHOR'S CONTRIBUTION

AJUC and RM conceptualized the project and methodology. RM performed the data collection, sample analysis, data analysis, validation, data curation and prepared the draft of the manuscript. JKR, RD, and DM supported during the analysis, writing of the manuscript and scientific discussions. ATM supported during the validation, during the scientific discussions and writing of the final manuscript. All authors contributed to the manuscript writing. All authors have read and approved the manuscript.

COMPETING INTERESTS

All the authors hereby declare that they have no competing interests.

ACKNOWLEDGEMENT

The authors are grateful to the support given by the Centre for Cheminformatics, Department of Chemistry, Malabar Christian College, Calicut, CSIR-OSDD Research Unit, IISc Campus, Bangalore, TATA CSIR-OSDD Fellowships and Open Source Pharma Foundation Bangalore. The authors also do recognize the support provided by Jadan Resnik in completion of this manuscript.

Table 1: The hydrogen bond donor and acceptor substituent's, part of virtual derivative series

Sl. No.	Molecules	Substituent
1	Zero donor acyclic	-CH ₂ -NH ₂
2	Zero donor cyclic	-CH ₂ -NH ₂
3	Poor donor acyclic	-CH ₂ -C(=O)-NH ₂
4	Poor donor cyclic	-CH ₂ -C(=O)-NH ₂
5	Moderate donor acyclic-1	-CH ₂ -C(=O)-NH-C ₆ H ₅
6	Moderate donor cyclic-1	-CH ₂ -C(=O)-NH-C ₆ H ₅
7	Moderate donor acyclic-2	-CH ₂ -C(=S)-NH-C ₆ H ₅
8	Moderate donor cyclic-2	-CH ₂ -C(=S)-NH-C ₆ H ₅
9	Good donor acyclic-1	-C ₆ H ₄ -OH
10	Good donor cyclic-1	-C ₆ H ₄ -OH
11	Good donor acyclic-2	-CH ₂ -C(=O)-NH-OH
12	Good donor cyclic-2	-CH ₂ -C(=O)-NH-OH
13	Strong donor acyclic	-C ₆ H ₂ -Cl ₂ -OH
14	Strong donor cyclic	-C ₆ H ₂ -Cl ₂ -OH
15	Very strong donor acyclic-1	-C(Cl ₂)-C(=O)-OH
16	Very strong donor cyclic-1	-C(Cl ₂)-C(=O)-OH
17	Very strong donor acyclic-2	1H-tetrazole-5-yl
18	Very strong donor cyclic-2	1H-tetrazole-5-yl
19	Proton acceptor zero acyclic	-CH ₂ -C(=O)-O-CH ₃
20	Proton acceptor zero cyclic	-CH ₂ -C(=O)-O-CH ₃
21	Moderate proton acceptor acyclic	-CH ₂ -C(=O)-CH ₃
22	Moderate proton acceptor cyclic	-CH ₂ -C(=O)-CH ₃
23	Very strong proton acceptor acyclic	1H-imidazol-1-ylmethyl
24	Very strong proton acceptor cyclic	1H-imidazol-1-ylmethyl

Table 2: Molecular mechanics, Semi-empirical calculations of virtual derivative series

Acyclic compound substituent R	Cyclic compound substituent R	Molecules	Energy MM+	Energy PM3	Energy AM1	Bond	Angle	Dihedral	VDW	Stretch bend	Electrostatic
-CH ₂ -NH ₂		Zero donor acyclic	3.67	-2765.75	-2791.28	0.29	1.94	1.055	2.95	0.22	2.78
	-CH ₂ -NH ₂	Zero donor cyclic	16.32	-2768.39	-2785.37	0.32	6.70	7.41	3.50	0.35	-1.90
-CH ₂ -C(=O)-NH ₂		Poor donor acyclic	2.52	-3037.09	-3065.61	0.43	2.31	3.25	3.38	0.26	-7.12
	-CH ₂ -C(=O)-NH ₂	Poor donor cyclic	8.57	-3041.89	-3060.81	0.41	6.50	8.54	3.97	0.36	-11.21
-CH ₂ -C(=O)-NH-C ₆ H ₅		Moderate donor acyclic-1	4.97	-4239.98	-4261.16	0.56	6.74	-1.96	6.77	0.26	-7.39
	-CH ₂ -C(=O)-NH-C ₆ H ₅	Moderate donor cyclic-1	16.89	-3971.49	-3982.31	0.49	10.27	14.99	9.63	0.27	-18.77
-CH ₂ -C(=S)-NH-C ₆ H ₅		Moderate donor acyclic-2	14.48	-4175.97	-4210.42	0.53	7.91	0.19	6.57	0.30	0.64
	-CH ₂ -C(=S)-NH-C ₆ H ₅	Moderate donor cyclic-2	25.46	-4178.08	-4205.98	0.58	11.37	6.19	7.46	0.40	-0.54
--C ₆ H ₄ -OH		Good donor acyclic-1	8.09	-3638.44	-3663.74	0.46	2.91	-2.66	7.98	0.20	-0.79
	-C ₆ H ₄ -OH	Good donor cyclic-1	17.807	-3631.94	-3662.93	0.54	7.39	3.31	8.60	0.27	-2.30
-CH ₂ -C(=O)-NH-OH		Good donor acyclic-2	5.68	-3101.4	-3129.4	0.40	2.02	0.46	4.14	0.22	-1.56
	-CH ₂ -C(=O)-NH-OH	Good donor cyclic-2	8.19	-2828.65	-2847.13	0.29	6.13	6.07	4.99	0.29	-9.58

Table 3: Molecular mechanics, Semi-empirical calculations of virtual derivative series

Acyclic compound substituent R	Cyclic compound substituent R	Molecules	Energy MM+	Energy PM3	Energy AM1	Bond	Angle	Dihedral	VDW	Stretch bend	Electrostatic
-C6H2-Cl2-OH		Strong donor acyclic	9.64	-3603.38	-3627.61	0.574	2.92	-4.2	9.38	0.21	0.75
	-C6H2-Cl2-OH	Strong donor cyclic	18.19	-3603.96	-3623.89	0.599	7.31	2.20	9.63	0.31	-1.86
-C(Cl2)-C(=O)-OH		Very strong donor acyclic-1	8.255	-2942.05	-2958.15	0.69	2.83	1.5	4.17	0.3	-1.23
	-C(Cl2)-C(=O)-OH	Very strong donor cyclic-1	8.96	-2946.11	-2965.	0.6	4.05	1.073	4.89	0.28	-1.93
1H-tetrazole-5-yl		Very strong donor acyclic-2	13.36	-2855.59	-2853.87	0.52	15.96	1.77	3.98	-0.06	-8.81
	1H-tetrazole-5-yl	Very strong donor cyclic-2	6.63	-2864.43	-2859.4	0.703	11.77	5.37	3.63	-0.48	-14.37
-CH2-C(=O)-O-CH3		Proton acceptor zero acyclic	5.8	-3364.85	-3329.87	0.41	2.41	-0.59	5.43	0.25	-2.1
	-CH2-C(=O)-O-CH3	Proton acceptor zero cyclic	14.26	-3251.43	-3279.1	0.36	7.15	5.05	5.62	0.38	-4.3
-CH2-C(=O)-CH3		Moderate proton acceptor acyclic	7.884	-3145.53	-3167.8	0.41	1.85	1.45	3.82	0.21	0.16
	-CH2-C(=O)-CH3	Moderate proton acceptor cyclic	14.16	-3151.15	-3172.78	0.36	5.93	6.26	3.88	0.32	-2.61
1H-imidazol-1-ylmethyl		Very strong proton acceptor acyclic	7.701	-3400.3	-3401.58	0.342	11.44	3.26	2.76	0.15	-10.25
	1H-imidazol-1-ylmethyl	Very strong proton acceptor cyclic	20.55	-3405.48	-3400.34	0.34	15.05	8.80	3.2	0.29	-7.12

Table 4: Molecular mechanics MM+, Semi-empirical PM3 and AM1 results and properties of experimentally validated compounds

	Molecules	Energy MM+	Energy AM1	Bond	Angle	Dihedral	VDW	Stretch bend	Electro static	CCI	HF
	Acyclic D mannose oxime (MO)	5.0137	-0.403	0.294	1.25	0.622	3.03	0.21	0.39	281145.9	-222.51
	Cyclic D mannose oxime (MO)	17.98	-0.40	0.29	5.61	6.55	4.28	0.311	0.94	311666.8	-221.85
	Acyclic N-mannopyranosylsemicarbazide (MPS)	-0.23	-0.367	0.33	2.45	2.05	2.96	0.25	-8.27	369219.1	-230.63
	Cyclic N-mannopyranosyl semicarbazide (MPS)	6.71	-0.4	0.38	6.42	8.16	4.55	0.37	-13.17	413621.7	-232.64
	Acyclic N-phenylmanno pyranosylamine (PMS)	7.77	-0.32	0.43	2.36	-2.63	8.10	0.24	-0.72	410127.8	-186.82
	Cyclic Acyclic N-phenylmanno pyranosylamine (PMS)	17.44	-0.34	0.53	6.92	3.35	8.70	0.29	-2.36	448677.5	-180.79
	Acyclic N-p chlorophenyl manno pyranosylamine (CMA)	8.64	-0.34	0.43	2.44	-2.67	8.46	0.23	-0.26	442628.1	-193.35
	Cyclic N-p chlorophenyl manno pyranosylamine (CMA)	17.93	-0.35	0.55	7.05	3.29	8.93	0.31	-2.2	483259.9	-187.8

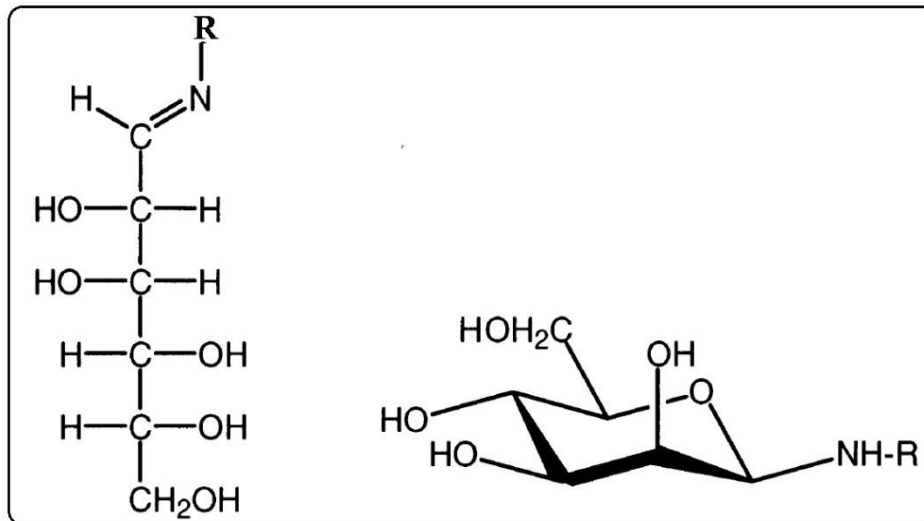


Fig. 1: Acyclic and Cyclic Conformations of D-mannose Schiff Base

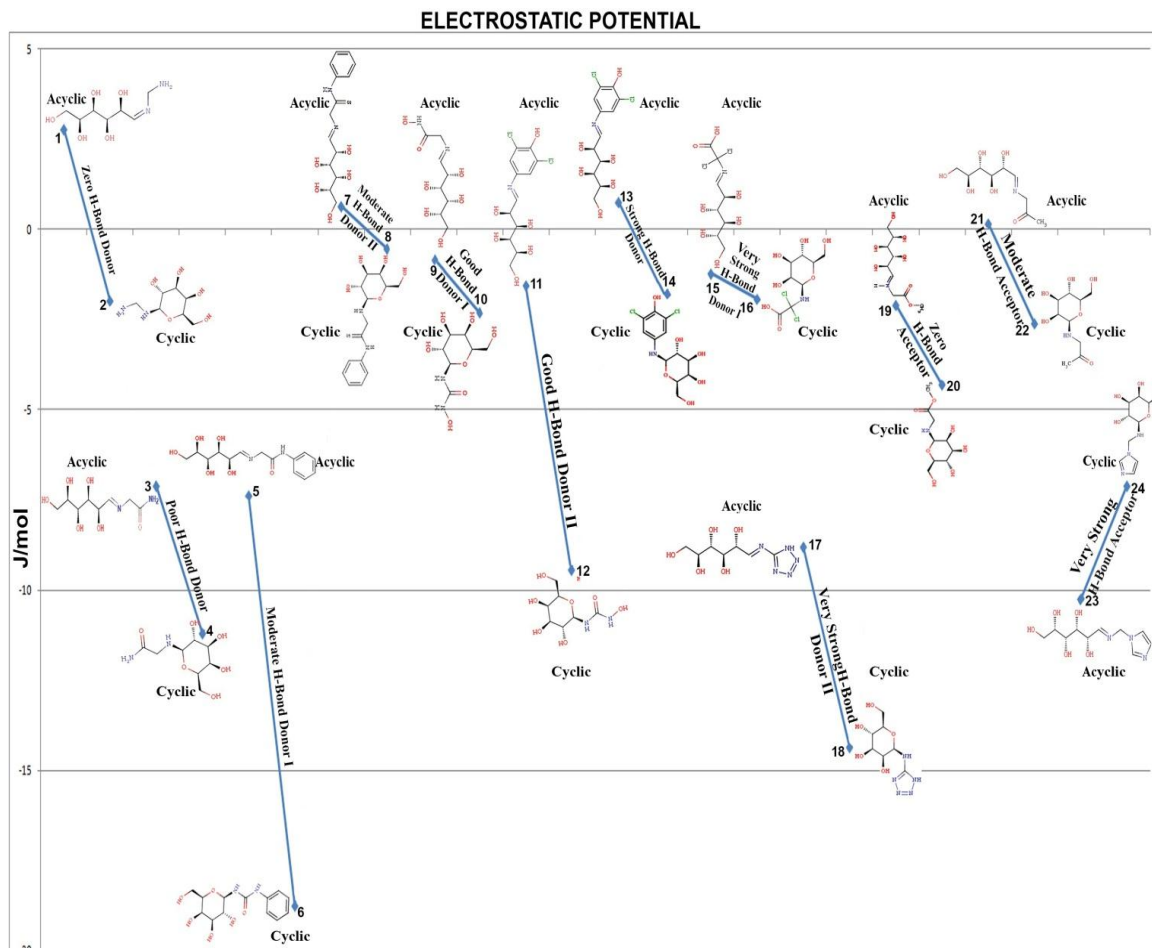


Fig. 2: Virtual Derivative Series - Gradation in Electrostatic Energy

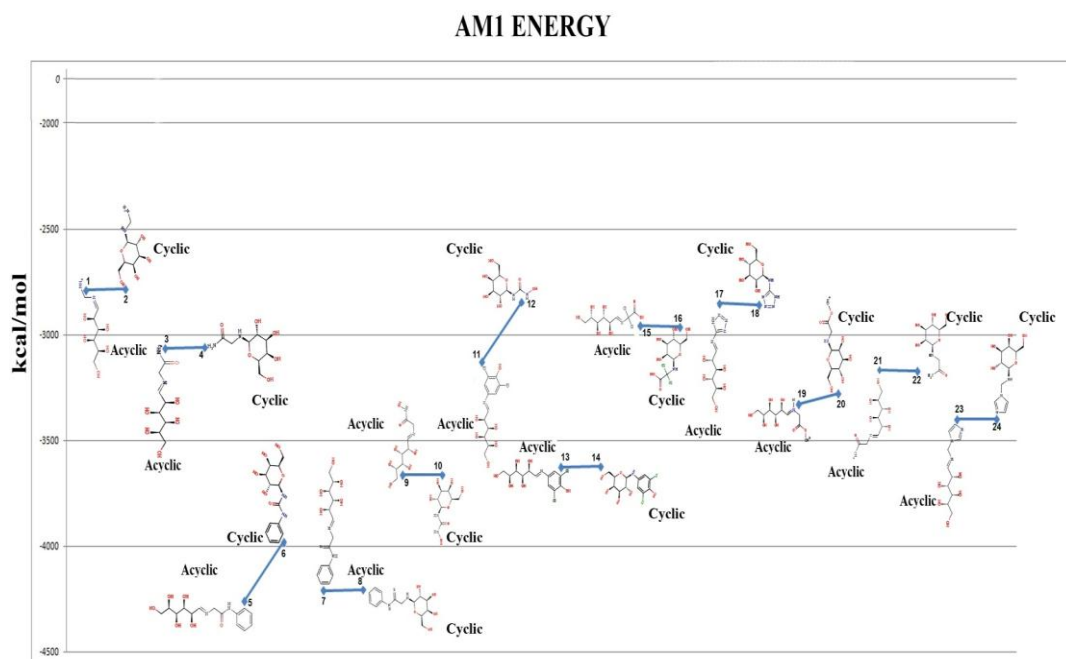


Fig. 3: Virtual Derivative Series - Gradation in AM1 Energy

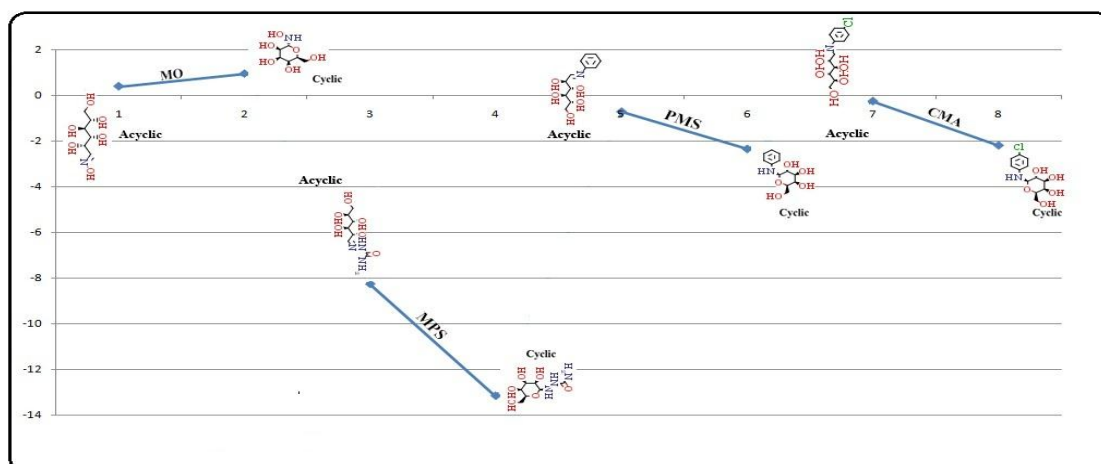


Fig. 4: Probe Molecules - Gradation in Electrostatic Energy

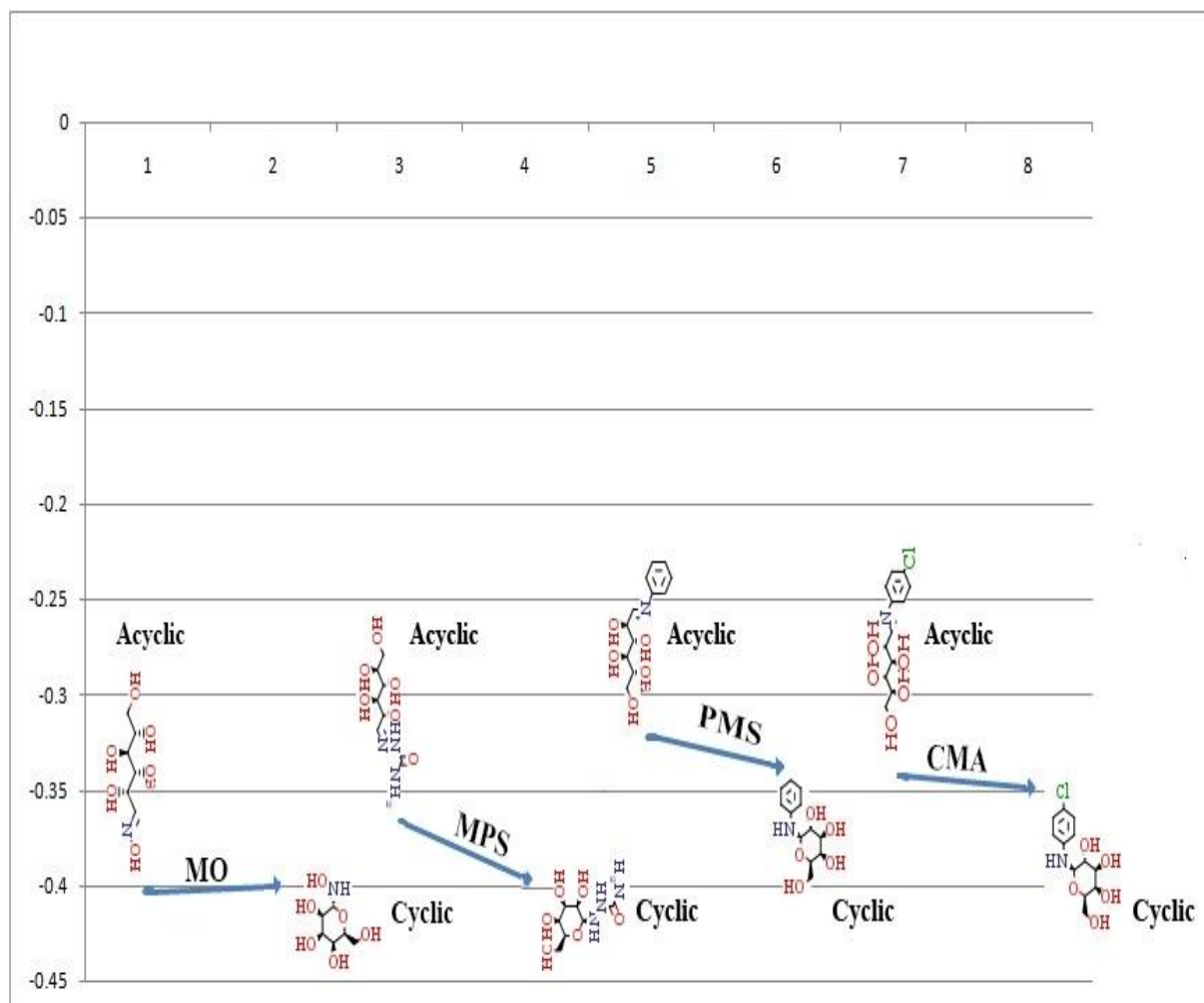


Fig. 5: Probe Molecules - Gradation in AM1 Energy

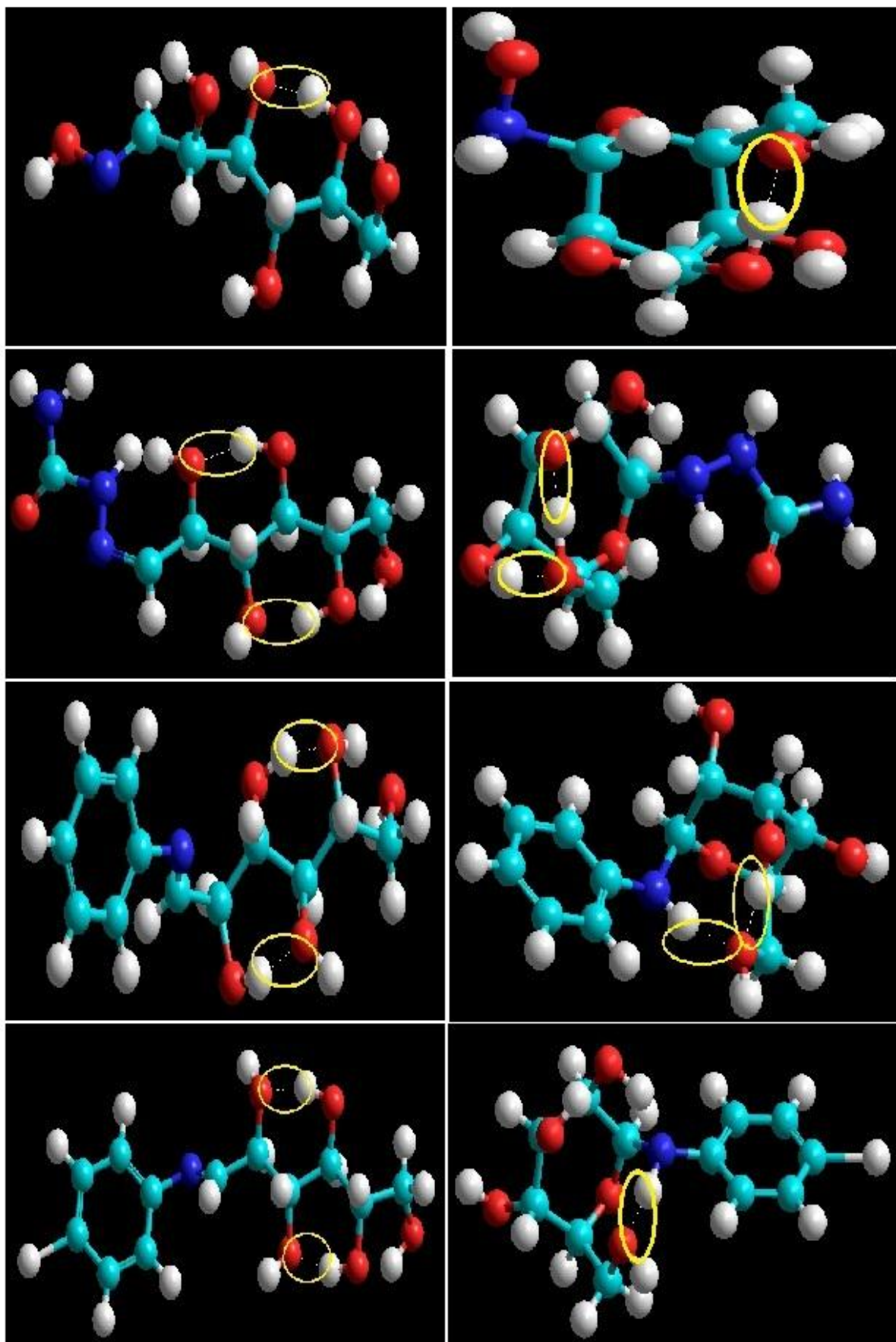


Fig. 6: Probe Molecules - Intramolecular Hydrogen Bonds

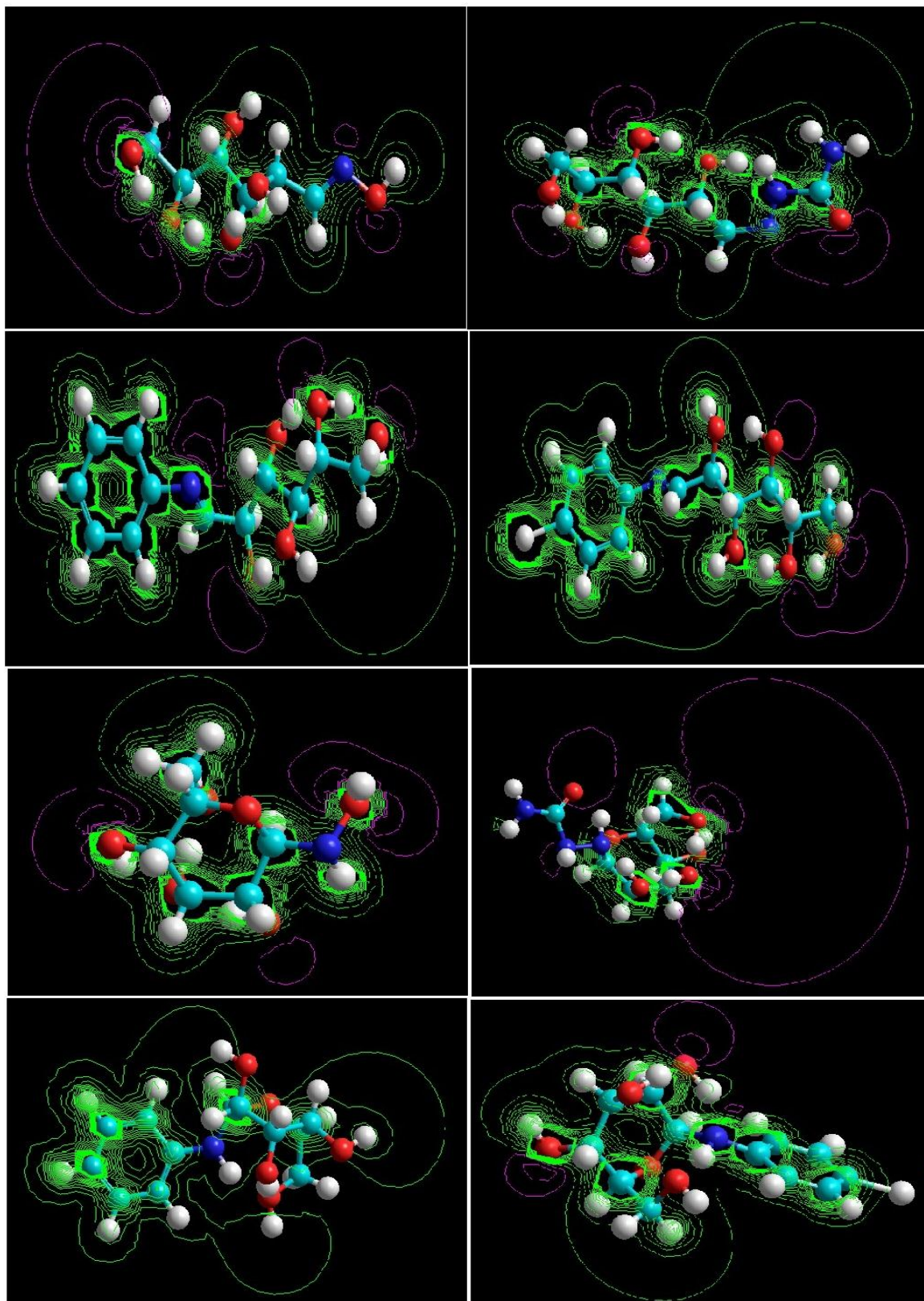


Fig. 7: Probe Molecules - Electrostatic 2D Contour Maps

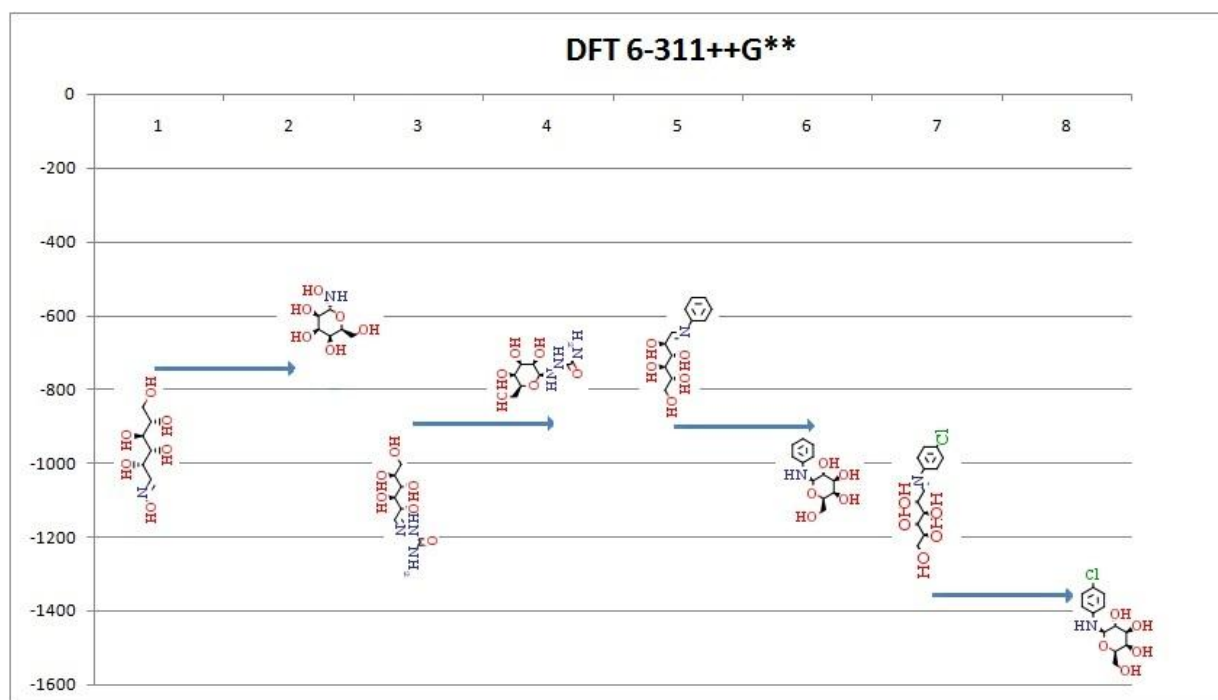


Fig. 8: Probe Molecules - DFT 6-311++G** Energy

REFERENCES

- Karno NG, Ratnasamy S and Walsh PJ. Synthesis of homochiral pentadentate sulfonamide-based ligands. *Tetrahedron: Asymmetry*. 2001;12(1):1719–1722.
- Genet JP, Ferroud D, Juge S and Montes JR. Synthesis of α -amino acids. Schiff base of glycine methyl ester. A new and efficient prochiral nucleophile in palladium chiral catalytic allylation *Tetrahedron Lett*. 1986;27(38):4573-4576. [http://dx.doi.org/10.1016/S0040-4039\(00\)85006-6](http://dx.doi.org/10.1016/S0040-4039(00)85006-6)
- Chatterjee D, Mitra A and Shepherd R. Oxo-transfer catalysis from t-BuOOH with C–H bond insertion using tridentate Schiff-base-chelate complexes of ruthenium(III). *Inorganica Chimica Acta*. 2004;357(4):980-990.
- Erskine PT, Newbold R, Roper J, Coker A, Warren MJ, Shoolingin-Jordan PM, Wood SP and Cooper JB. The schiff base complex of yeast 5-aminolaevulinic acid dehydratase with laevulinic acid. *Protein Science*. 1999;8(6):1250–1256. <http://dx.doi.org/10.1110/ps.8.6.1250>
- Cad VT. Gossypol and its new derivatives: Synthesis and study of Biological Activities [Thesis]. Inst of Chemistry of Natural Substances: University of Paris; 2002.
- Verma M, Pandeya SN, Singh KN and Stables JP. Anticonvulsant activity of Schiff bases of isatin derivatives. *Acta Pharm*. 2004;54(1):49-56.
- Toshihiko T, Arnd B, Cindy MQ, Melvin IS, Thomas JM and Harry BG. Selective Inhibition of Human α -Thrombin by Cobalt(III) Schiff Base Complexes. *J Am Chem Soc*. 1998;120(33):8555-8556. <http://dx.doi.org/10.1021/ja981191x>
- Kabir AKMS, Matin MM, Bhuiyan MMR and Rahim MA. Synthesis and characterization of some acylated derivatives of D-mannose. *The Chittagong Univ J Sci*. 2001;25:65-73.
- Kabir AKMS, Matin MM and Sanaullah AFM. Regioselective synthesis and characterization of some lyxose derivatives. *Ceylon J Sci*. 2002;9:9-14.
- Kabir AKMS, Matin MM, Alam MJ and Manchur MA. Synthesis and antimicrobial activities of some D-glucose derivatives. *J Bangladesh Chem Soc*. 2000;13:107-115.
- Ojala WH, Ostman JM and Ojala CR. Schiff bases or glycosylamine crystal and molecular structures of four derivatives of D-mannose. *Carbohydr Re*. 2000;326(2):104–1129. [http://dx.doi.org/10.1016/S0008-6215\(00\)00026-4](http://dx.doi.org/10.1016/S0008-6215(00)00026-4)
- Peter C, Trevor WH and Martin B. Molecular modeling of inorganic compounds. 3rd edition. WILEY-VCH Verlag GmbH & Co.

- 2009.<http://dx.doi.org/10.1002/9783527628124>.
13. Allinger NL. MM2 A Hydrocarbon Force Field Utilizing V1 and V2 Torsional Terms. *J Am Chem Soc.* 1977;99(25):8127-8134.
 14. Hyper Chem Computational Chemistry, Hypercube Inc. 1996.HC50-00-03-00.
 15. Vanommeslaeghe K, Guvench O and MacKerell AD Jr. Molecular Mechanics. *Curr Pharm Des.* 2014;20(20):3281-3892.
 16. Thiel W and Voityuk A. Extension of the MNDO formalism to d orbitals: Integrals approximations and preliminary numerical results. *Theor Chim Acta.* 1992;81(6):391-404.
<http://dx.doi.org/10.1007/BF01134863>
 17. Thiel W and Voityuk A. Extension of MNDO to d orbitals: Parameters and results for the halogens. *Int J Quantum Chem.* 1992;44(5):807-829.
<http://dx.doi.org/10.1002/qua.560440511>
 18. Manuel AOM. Scope of computational organometallic chemistry: Structure, reactivity and properties [Thesis]. University of Autonomia de Barcelona; 2014.
 19. HyperChem (TM) Professional 8.0. Hypercube Inc. 1115 NW 4th Street, Gainesville, Florida-32601, USA.
 20. Choe JI, Kwangho K and Chang SK. Molecular Modeling of Complexation of Alkyl Ammonium Ions by p-tert-butylcalix[4]crown-6-ether. *Bull Korean Chem Soc.* 2000;21(5):465-470.